IEEE Access
Multidisciplinary ⋮ Rapid Review ⋮ Open Access Journal

Received 4 July 2025, accepted 12 July 2025, date of publication 17 July 2025, date of current version 24 July 2025.

Digital Object Identifier 10.1109/ACCESS.2025.3590069

RESEARCH ARTICLE

Study of Optimal Base Station Deployment for UAM Operations in an Urban Environment Based on a Genetic Algorithm

MINSANG YOON, JISEOK PARK, BOSUNG PARK, TAEKYEONG JIN, AND HOSUNG CHOO, (Senior Member, IEEE)
Department of Electronic and Electrical Engineering, Hongik University, Seoul 04066, South Korea

Corresponding author: Hosung Choo (hschoo@hongik.ac.kr)

This work was supported in part by Korea Research Institute for Defense Technology Planning and Advancement (KRIT) Grant funded by Korean Government (Defense Acquisition Program Administration-DAPA), (Space Signal Intelligence Research Laboratory), in 2022, under Grant KRIT-CT-22-021.

ABSTRACT In this paper, we propose a method for determining the optimal base station deployment to establish a stable communication environment for urban air mobility (UAM) operation in urban areas. To realistically model the UAM operating environment, we utilize DEM files that include data on terrain and buildings. Furthermore, the radiation patterns of the BS's antenna are generated according to the 3GPP-standard, and the receiver antenna patterns are obtained through analysis of the UAM's mounted antenna. The proposed method uses binary chromosomes to determine the locations of BSs and the orientations of the antennas. A genetic algorithm is then used to determine the optimal deployment of the base stations. When applying the proposed method to optimize BS deployment in the UAM corridor (area of approximately 5.4 km^2), the optimization process resulted in the deployment of two base stations at 3.5 GHz, achieving an average received power of −61.36 dBm across the corridor. At 5.4 GHz, three base stations are deployed, with an average received power of −63.74 dBm. To validate the reliability of the simulation, measurements are conducted in a real urban environment, comparing the results from measurement, theory, and simulation. The received power values obtained from measurement, theory, and simulation are − 110.21 dBm, −110.82 dBm, and −110.38 dBm, respectively. These results demonstrate that the proposed BS deployment method can be used to establish a stable communication environment in a real UAM corridor.

INDEX TERMS Urban air mobility, base station deployment, genetic algorithm, electromagnetic wave propagation, ray-tracing.

I. INTRODUCTION

Urban air mobility (UAM) has recently emerged as an innovative solution to alleviate traffic congestion by utilizing low-altitude airspace [1]. In order to commercialize UAM, establishing a stable communication network between UAM operating at altitudes of 300 m to 600 m and ground base stations (BSs) is required [2]. To ensure stable command and control communications, ground BSs specifically designed for UAM, rather than those intended for terrestrial users such as pedestrians or vehicles, must be deployed [3], [4], [5]. In urban environments, non-line of sight (NLOS) conditions and multipath interference caused by high-rise buildings can impact communication reliability and quality [6]. Previous studies have utilized empirical models, such as the Okumura and COST-231 Hata models [7], [8], [9], to analyze the radio propagation environment of complex urban areas [10]. These models do not consider the reflection, diffraction, and scattering that occur in urban environments and they also have limitations in the frequency bands that can be analyzed. To address these issues, previous studies have utilized the ray-tracing method in combination with learning-based prediction and the ITU-R P.1238 model to analyze radio propagation environments [11], [12]. However, these studies

The associate editor coordinating the review of this manuscript and approving it for publication was Walid Al-Hussaibi.

do not account for variations in received power due to altitude changes, nor do they propose optimization algorithms for BS deployment. Some studies have reported that BS deployment can be determined using the alternating direction method of multipliers (ADMM) [13]. In this approach, the ray-tracing method is not utilized for radio propagation analysis during the optimization process. Therefore, determining BS deployment solutions for stable UAM communication requires modeling the urban environment, including UAM corridors and altitude variations, and comprehensively analyzing these factors by combining ray-tracing simulation with an optimization algorithm [14].

In this paper, we propose a method for determining the optimal BS deployment to establish a stable communication environment for UAM in urban areas [15]. We analyze NLOS conditions and multipath interference in urban environments, by modeling actual terrain and buildings and applying them to the ray-tracing based electromagnetic (EM) simulator Wireless InSite [16]. In our analysis, receivers are placed along the UAM corridor, and building rooftops currently hosting mobile communication BSs are selected as candidate sites for BS deployment. These rooftops are selected to minimize the impact of LOS blockage by buildings. In order to determine the optimal BS deployment, a genetic algorithm (GA) is utilized [17], with each potential location represented as a binary chromosome for GA input data [18]. In addition, the transmit antenna patterns used in Wireless InSite are based on the mobile communication BS standards provided by 3GPP [19], [20], and the receive antenna pattern is obtained from mounted analysis with XPENG's UAM model, X2, through CST simulation software [21]. By using this approach, a radio propagation environment similar to the actual UAM operational environment is modeled in Wireless InSite [22], and BS deployment can be optimized through the GA based on the simulated received power data from receivers placed along the UAM corridor. By utilizing the proposed method, the optimal number of BSs for the Yeouido UAM corridor is determined to be 2 for the 3.5 GHz band and 3 for the 5.4 GHz band to establish a stable communication environment. While approximately six microcell base stations are required to cover the 5.4 km^2 corridor using conventional deployment [23], the proposed optimization achieves full coverage with only two 3.5 GHz and three 5.4 GHz base stations, demonstrating the potential for significant cost savings. To verify the accuracy of the simulation results and the feasibility of the proposed BS deployment method, we set up a measurement system in the real urban environment along the Han River in Seoul [24]. The received power measurements are compared with the theoretical and simulation results.

The paper is organized as follows. In Section II, we model the Yeouido UAM corridor environment by integrating high-resolution terrain and building data into the Wireless InSite simulator and establish criteria for BS location selection and antenna orientation. In Section III, we formulate the BS deployment problem as a cost function-based genetic algorithm, present the corresponding pseudocode, and validate the optimized layouts via trajectory-based simulations and on-site measurements. In Section IV, we conclude the paper by summarizing key findings, discussing their feasibility for UAM communication network planning, and outlining directions for future work.

II. MODELING OF UAM OPERATIONAL ENVIRONMENT

Figure 1 illustrates the urban operating environment of UAM and its wireless communication scenario. The UAM travels along a fixed corridor at altitudes of 300 m to 600 m as outlined in the Korea-UAM Concept of Operations 1.0 [25], and the locations of the directional BSs are required to support a stable communication network between BSs and aircraft. Failure to take into account urban terrain and buildings when selecting locations for new BSs can obstruct the propagation of EM waves or lead to multipath interference. This interference can diminish the received power of the UAM, impacting communication quality. Furthermore, shaded areas that occur due to the received power being below the receiver sensitivity can result from increased path loss with an insufficient number of BSs. This can lead to the degradation of UAM communication and operation. By contrast, deploying an excessive number of BSs can result in frequency energy waste and economic losses due to installation costs. Therefore, to determine an optimal number and localization of BSs, the analysis of radio propagation environment in urban areas is required in relation to the number and location of the BSs in advance.

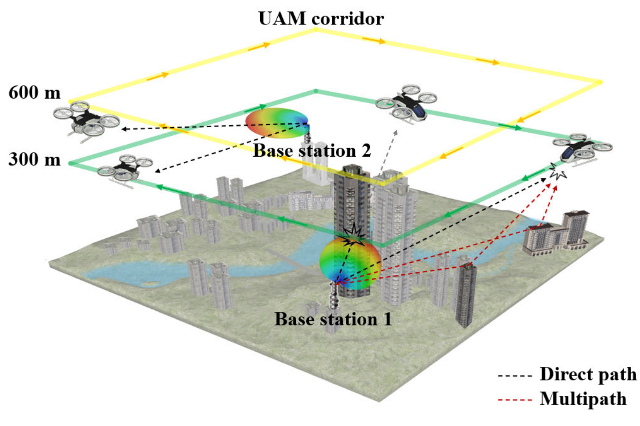

FIGURE 1. UAM communication in dense urban environments.

Figure 2 represents the planned UAM corridor and the modeled surrounding urban environment in the EM simulator. The terrain and buildings near the Han River are modeled in the ray-tracing EM simulator, Wireless InSite, to enhance analysis accuracy. The UAM operating corridor along the Han River in Seoul, South Korea, can be observed, as shown in Figure 2(a). Within this corridor, the UAM operates at altitudes ranging from 300 m to 600 m along a fixed route at points P-2 to P-6, which are part of the entire corridor. The urban environment surrounding the corridor is modeled using Wireless InSite, as shown in Figure 2(b). This modeling is required to establish a realistic radio environment and optimize BS deployment to support stable communications between BSs and aircraft. In this process, we use the building location and digital elevation model (DEM) data provided by the Ministry of Land, Infrastructure and Transport (MOLIT) of Korea [26]. To minimize the impact of DEM data errors on received power estimation, a 1 m resolution terrain dataset is employed. Through preliminary experiments, we confirmed that when the ground elevation errors in the DEM data exceed 5 m, the optimal BS deployment and the resulting average received power across the corridor may vary. The building material is set to concrete ($\varepsilon_r = 7$, $\sigma = 0.015$ S/m), the ground to wet earth ($\varepsilon_r = 25$, $\sigma = 0.02$ S/m), and the Han River to water ($\varepsilon_r = 81$, $\sigma = 0.22$ S/m).

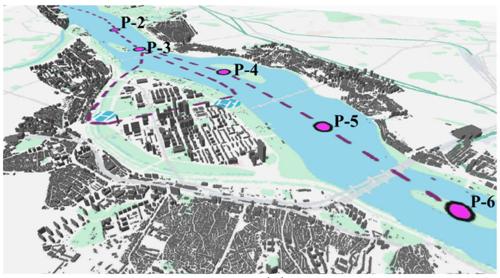

(a)

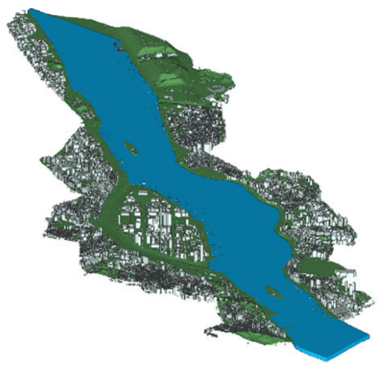

(b)

FIGURE 2. UAM urban environment modeling. (a) UAM corridor on the Han River, Korea. (b) Urban environment modeling in Wireless InSite.

Figure 3 shows the base station candidates (BS_{cand}) at potential locations for deploying BSs in urban environments, as well as the placement of receivers (Rx) along the UAM corridor. Ground BSs are positioned at the highest point among the surrounding buildings to ensure reliable communication with aircraft. Since these building rooftops are used for conventional BSs, they can be selected as potential locations for BS deployment. In our analysis, a total of 128 potential BS locations, represented by green cubes in the figure, are selected to minimize the propagation blockage and interference caused by complexity of urban environments. The receivers, shown as red cubes in the figure, are arranged to calculate the received power of the UAM assumed to be operating within the corridor. A total of 1,024 receivers are deployed at altitudes ranging from 300 m to 600 m, with 100 m increments. At each altitude, the receivers are spaced 70 m apart. The 3D position coordinates of the BS_{cand} and Rx serve as input to the GA that is effective at locating the global optimum within complex, nonlinear, and discrete search spaces [27], [28], [29].

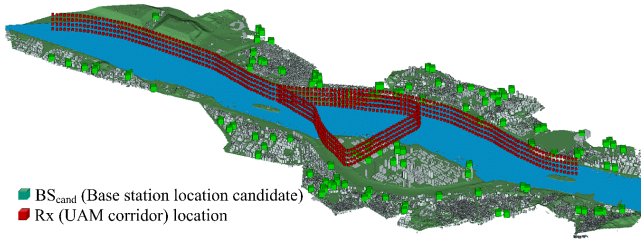

FIGURE 3. Number labeling on base station locations and UAM receiving positions.

Figure 4 illustrates the method used to label the numbers of BS_{cand} and Rx locations and to determine the radiation direction of the BS. In order to optimize BS deployment, Wireless InSite is combined with the GA and the chromosomes of the GA are represented in binary data. The numbers are labeled sequentially to the potential BS locations, as shown in Figure 4(a). For the corridor Rx, sequential numbers are also labeled, with 256 receivers per one altitude at 100 m intervals from 300 m to 600 m. The binary chromosomes consist of the potential BS_{cand} numbers and the Rx numbers, as shown in Figure 4(b). The upper 7 bits of the chromosome, shown in green, represent the labeled numbers of 128 potential BS locations, while the lower 10 bits, represented in red, correspond to the labeled numbers of 1,024 Rx deployed within the corridor. These 17 bits are represented as a one-to-one correspondence with the 3D position coordinates of BS_{cand} and Rx within the simulation. To determine the BS radiation angle, the BS_{cand} presented by the upper 7 bits in a chromosome is directed towards the Rx represented by the lower 10 bits. Therefore, the information pair consisting of the BS location and radiation direction is uniquely determined by a single chromosome. The radiating elevation angle and azimuth angle of the BS are calculated using the following equation [30]:

$$\theta_{Elevation} = \tan^{-1}\left(\frac{z_{Rx} - z_{Tx}}{\sqrt{(x_{Rx} - x_{Tx})^2 + (y_{Rx} - y_{Tx})^2}}\right) \quad (1)$$

$$\theta_{Azimuth} = \tan^{-1}\left(\frac{y_{Rx} - y_{Tx}}{x_{Rx} - x_{Tx}}\right) \quad (2)$$

where (x_{Tx}, y_{Tx}, z_{Tx}) and (x_{Rx}, y_{Rx}, z_{Rx}) refer to the 3D coordinates of the Tx (subscript Tx indicates a selected BS_{cand} as a BS location) and Rx, respectively, corresponding to the 17-bit chromosome, with coordinate values in meters (m). By using this coordinate information, the elevation and azimuth angles are calculated, allowing BS antennas to be directed toward the corridor to minimize shaded areas. This process enables the GA to search for the optimal solution in determining the locations of BSs and their radiation directions.

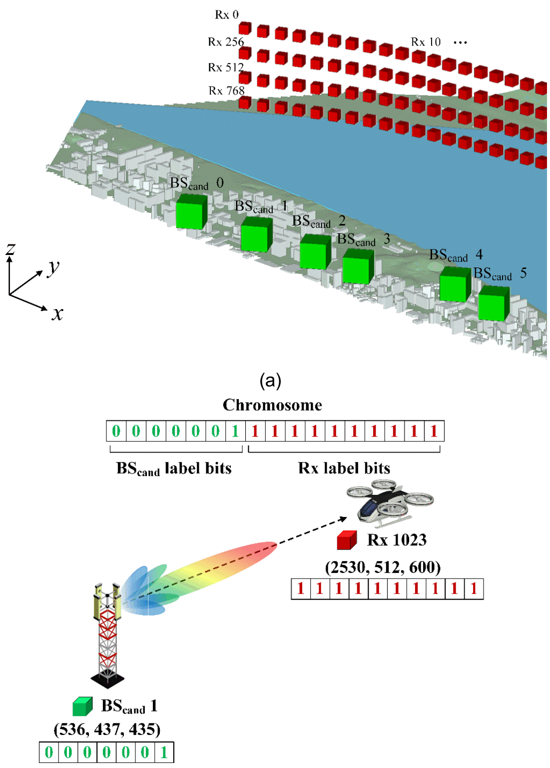

FIGURE 4. Preprocessing for BS deployment determination. (a) Number labeling on BS_{cand} and Rx positions. (b) Determination method of BS location and radiating direction.

Figure 5 presents the BS antenna patterns used for analyzing urban radio propagation in the operating bands of in-flight entertainment (IFE) and air traffic control (ATC) in UAM scenarios. The BS antenna pattern for each band is generated in the EM simulator CST, and a 1 × 8 linear array of patch antennas is utilized to comply with the ground BS antenna pattern standards provided by 3GPP [31]. The ground BS antenna is required to be directed toward the airspace to ensure stable communication between the ground BS and the UAM, as shown in Figure 5(a). In addition, a fan beam antenna pattern is required to establish a wide-area communication environment [32]. The radiation patterns of fan beam antennas operating at 3.5 GHz for the IFE band are observed in the *zx*-plane and *zy*-plane, as shown in Figure 5(b). The antenna pattern is designed with a bore-sight gain of 16.7 dBi, an SLL of 21.7 dB, and a 3 dB beamwidth of 10.0° in the elevation direction and 71.6° in the azimuth direction. The radiation patterns of the fan beam antenna operating at 5.4 GHz for the ATC band are provided in the *zx*-plane and *zy*-plane, as shown in Figure 5(c). The antenna pattern is designed with a bore-sight gain of 16.8 dBi, and an SLL of 22.5 dB, and a 3 dB beamwidth of 10.0° in the elevation direction and 70.9° in the azimuth direction.

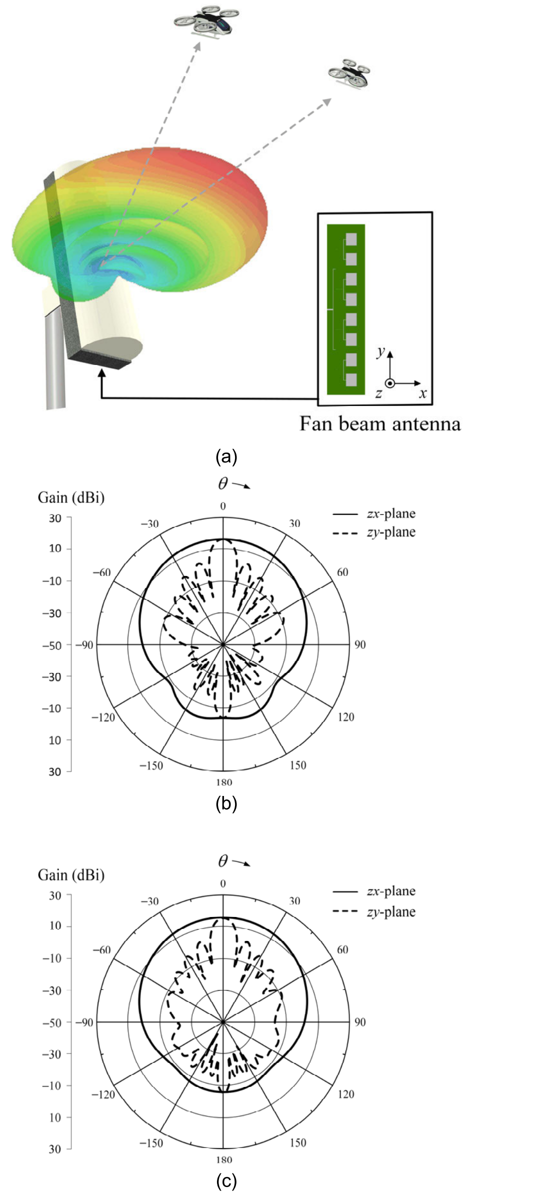

FIGURE 5. Fan beam antenna patterns designed with 1 × 8 patch array. (a) 3.5 GHz fan beam antenna patterns. (b) 5.4 GHz fan beam antenna patterns.

Figure 6 provides the radiation patterns of the UAM-mounted monopole receiver antenna. To analyze a more realistic radio environment for UAM operation, modified monopole antenna patterns due to structures such as the UAM's landing gear and propellers are applied in Wireless InSite. The potential UAM model selected is the Voyager X2 of XPENG [33], and the 3D EM model of the aircraft is applied in CST, as shown in Figure 6(a). A simulation is performed by mounting a monopole antenna at the location where the receiving antenna is installed on the X2. The radiation patterns of the mounted monopole antenna operating at 3.5 GHz are observed in the *zy*-plane and *xy*-plane, as shown in Figure 6(b). The patterns exhibit a maximum gain of 7.79 dBi at an angle of −119.0° in the *zy*-plane. The radiation patterns of the mounted monopole antenna operating at 5.4 GHz are also observed in the *zy*-plane and *xy*-plane, as shown in Figure 6(c). The patterns exhibit a maximum gain of 7.01 dBi at an angle of −114.0° in the *zy*-plane. The antenna patterns generated through this process are then applied to the Rx of the modeled corridor.

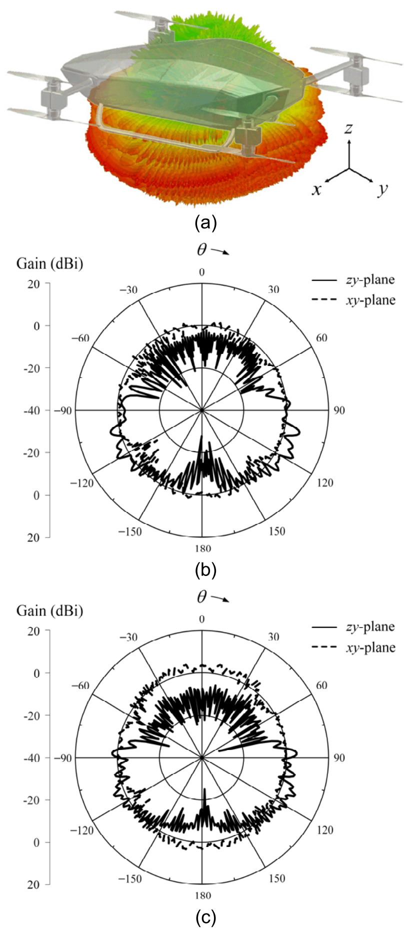

FIGURE 6. **Monopole antenna patterns mounted on UAM. (a) UAM 3D model and radiation patterns. (b) 3.5 GHz radiation patterns for *zx*-plane and *xy*-plane. (c) 5.4 GHz radiation patterns for *zx*-plane and *xy*-plane.**

III. BASE STATION DEPLOYMENT OPTIMIZATION USING GENETIC ALGORITHM

Figure 7 illustrates the detailed flowchart and pseudocode of the proposed BS deployment optimization method using the GA. To optimize BS deployment for UAM operations, the proposed GA is applied through the following process. In the first step, the GA randomly generates 17-bit chromosomes (Initialize_Population) that determine the BS and Rx coordinates corresponding to locations. Azimuth and elevation angles are calculated based on the determined locations, and the BS is deployed on the modeled map in Wireless InSite. The transmission power of the BS is set to 40 dBm, and an EM simulation is then conducted (RUNSIM) to calculate the received power at 1,024 Rx positioned in the corridor. The received power data (P_rx) from the Rx is used to calculate the cost function (i.cost) value of the GA using the following equation:

$$\text{Cost} = -P_{avg} + w \cdot N_{low} \quad (3)$$

where P_{avg} refers to the average received power (mean_rx) across all the Rx locations, and w is the weight for N_{low}(weak_count). N_{low} represents the number of Rx locations that are unable to communicate due to low received power below a sensitivity level of −103 dBm [34]. Since the GA reproduces the next generation to minimize the cost function value [35], the next generation of BS deployment can be updated to increase P_{avg} and decrease N_{low}. The weight w adjusts the decreasing convergence speed of the cost function value, preventing the algorithm from becoming trapped in a local optimum. By using this cost function, the BS chromosomes are updated to maximize the average received power in the corridor and minimize shaded areas. When all Rx satisfy the sensitivity requirement (−103 dBm), the algorithm terminates and returns the best-performing chromosome (Tx_best, Rx_best). Otherwise, if the maximum generation is reached without achieving full coverage, the number of BS (K) is incremented by one, and the optimization is repeated. This iterative process continues until the entire coverage area is satisfied with the minimal number of BS, ensuring both efficiency and stability in the UAM communication network. Using the procedure, we can obtain a fixed base station configuration that ensures all Rx points meet the minimum required received power during operation.

Table 1 presents the values of the GA hyperparameters implemented in the MATLAB environment [36]. The roulette wheel method, which increases the probability of passing down superior solutions to the next generation, is utilized as a method of selecting individuals to reproduce the next generation [37]. It assigns greater selection probability to individuals with lower cost function values. The number of generations in the GA is set to 30, with a crossover probability of 0.8. In particular, the path loss of EM waves at 5.4 GHz is greater than at 3.5 GHz [38], requiring a larger number of BSs and more computation. Therefore, the population and mutation rate are set to 30 and 0.1 at 3.5 GHz, while at 5.4 GHz, they are set to 40 and 0.15, respectively. The hyperparameters are selected within empirically validated ranges that ensure stable convergence and solution quality, while considering the trade-off between convergence speed and computational cost. In particular, GA-based optimization of cellular base station deployment, a population size of 20-50 and a mutation rate of 0.1-0.5 have been shown to be appropriate and effective [39]. By using the proposed GA hyperparameters, the algorithm prevents convergence to local optima and effectively searches for the global minimum.

Figure 8 represents the optimal BS deployment results for the UAM corridor in Yeouido, as determined by the proposed method. The BSs are placed to cover the shaded areas within the UAM corridor. In our analysis, an urban area of approximately 36.3 km^2 including the UAM corridor is modeled, and

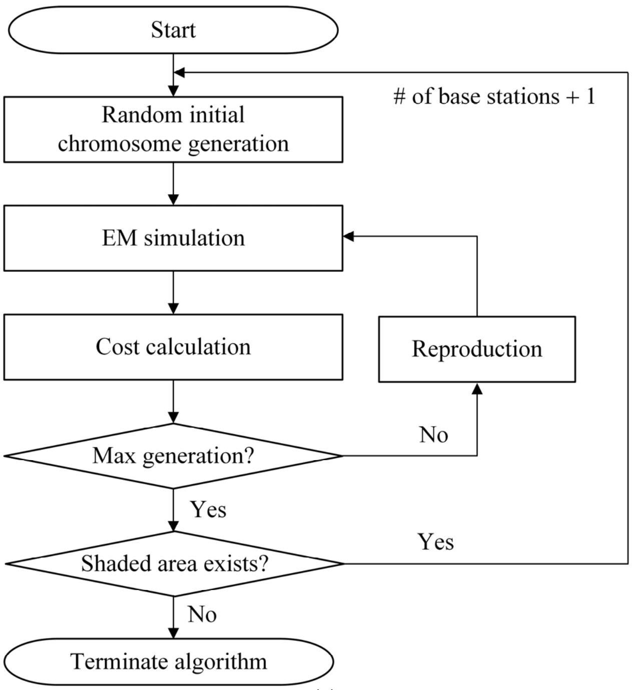

(a)

Algorithm: GA-Based Base Station Placement with Full Coverage Constraint

```
Input:
  C ← Candidate Tx locations
  R ← Rx grid points
  K ← Initial number of base stations (Starts from 1)
  G ← Number of generations per optimization
  N ← Population size
  M ← Mutation rate
  w ← Penalty weight for shaded areas
  Sensitivity ← Rx power threshold (−103 dBm)
Output:
  Tx_best ← Optimized base station positions
  Rx_best ← Optimized Rx coordinate within the aerial corridor
aligned with the BS's bore-sight
procedure GA_Optimize(C, R, K)
    repeat
      P ← Initialize_Population(N, C, K)
      for g = 1 to G do
        for each individual i in P do
          [Tx_i, Rx_i] ← Decode(i)
          P_rx ← RUNSIM(K, Tx_i, Rx_i)
          mean_rx ← mean(P_rx)
          weak_count ← count(P_rx ≤ Sensitivity)
          i.cost ← −mean_rx + w × weak_count
        end for
        P ← Selection_Roulette(P)
        P ← Crossover(P)
        P ← Mutation(P)
        Update_Best(P)
      end for
      [Tx_best, Rx_best] ← Decode(Best_Individual(P))
      P_rx_best ← RUNSIM(K, Tx_best, Rx_best)
      if all(P_rx_best > Sensitivity) then
        return Tx_best, Rx_best
      else
        K ← K + 1
      end if
    until false
end procedure
```

(b)

FIGURE 7. Base station deployment optimization process. (a) Block diagram of the GA optimization process. (b) Pseudocode of the optimization process using the GA.

TABLE 1. Hyperparameters of the GA.

Frequency	Selection method	Maximum generation	Crossover probability	Population	Mutation probability
3.5 GHz	Roulette wheel	30	0.8	30	0.1
5.4 GHz				40	0.15

BS optimization is performed assuming a total system loss of 8 dB for the Tx and Rx. The system loss is set to 8 dB in order to ensure reliable communication performance, considering the effects of UAM mobility-induced Doppler shifts, seasonal variations, and building material characteristics [40], [41], [42], [43]. When the number of BSs is optimized for the 3.5 GHz band, a stable communication environment is established with two BS, and the average received power of 1,024 Rx in the corridor is calculated as −61.36 dBm. The first BS (BS-1) is positioned at (661, −961, 48) on the map, and the Tx antenna is installed to orient towards an azimuth of 139.0° and an elevation of 5.3°. The second BS (BS-2), located at (1123, −1045, 59), is set to orient towards a −16.2° azimuth and a 6.1° elevation, as shown in Figure 8(a). Similarly, for the 5.4 GHz band, the optimal number of BS is three, with an average received power of −63.74 dBm across the 1,024 Rx in the corridor. The first BS (BS-1) is positioned at (441, 720, 49) with an azimuth of 161.2° and an elevation of 6.3°. The second BS (BS-2) is positioned at (−552, −1888, 68), with an azimuth of 34.8° and an elevation of 6.7°. The third BS (BS-3) is positioned at (1123, −1045, 59) with an azimuth of −36.6°, and an elevation of 56.8°, as shown in Figure 8(b). For a trajectory-based simulation, the variations in received power are calculated as the UAM travels along the corridor at a speed of 240 km/h. The received power from the 3.5 GHz BSs is evaluated as the UAM operates at altitudes of 300, 400, 500, and 600 meters, as shown in Figure 8(c). During the 270 second operation, the received power remains above the sensitivity (−103 dBm), ensuring stable communication. Following the same methodology used from the 3.5 GHz case, the received power from the 5.4 GHz BSs is analyzed while the UAM operates, as shown in Figure 8(d). The received power remains above the sensitivity threshold throughout the operation, confirming stable communication capability for the UAM.

Although computational complexity increases with larger urban areas, the modularity of the proposed framework ensures that the same optimization process can be repeatedly applied to segmented corridors. When optimizing BS deployment in a larger metropolitan area, the number of modules increases proportionally with the modeled urban area and total corridor length. By optimizing the BS deployment of each module in parallel, the overall computation time can be reduced more efficiently compared to sequential optimization. These results indicate that the required number of BSs may vary depending on the frequency within the same urban environment.

In addition, to verify the compatibility of the proposed framework with other optimization algorithms, additional experiments are conducted using PSO, DE, GWO, and ACO [44], [45], [46], [47] over 30 generations. The number of individuals per generation for all five algorithms is set to 30 and 40 for the 3.5 GHz and 5.4 GHz bands, respectively, as defined for the GA in TABLE 1. In this comparison, all optimized base station deployment results derived from the GA, PSO, DE, GWO, and ACO achieve full coverage without any shaded areas. For the 3.5 GHz band, the average received power in the corridor for each algorithm is −61.36 dBm, −62.29 dBm, −62.79 dBm, −61.75 dBm, and −61.80 dBm, respectively. In the case of the 5.4 GHz band, the average received power is −63.74 dBm, −64.76 dBm, −63.77 dBm, −63.75 dBm, and −64.30 dBm, respectively. The results indicate that the proposed optimization framework can be effectively applied across different metaheuristic algorithms, including GA, PSO, DE, GWO, and ACO. The minimum number of BSs required to satisfy the UAM sensitivity (−103 dBm) is consistent across all algorithms, with 2 BSs at 3.5 GHz and 3 at 5.4 GHz to support the stable communication environment for UAM operation.

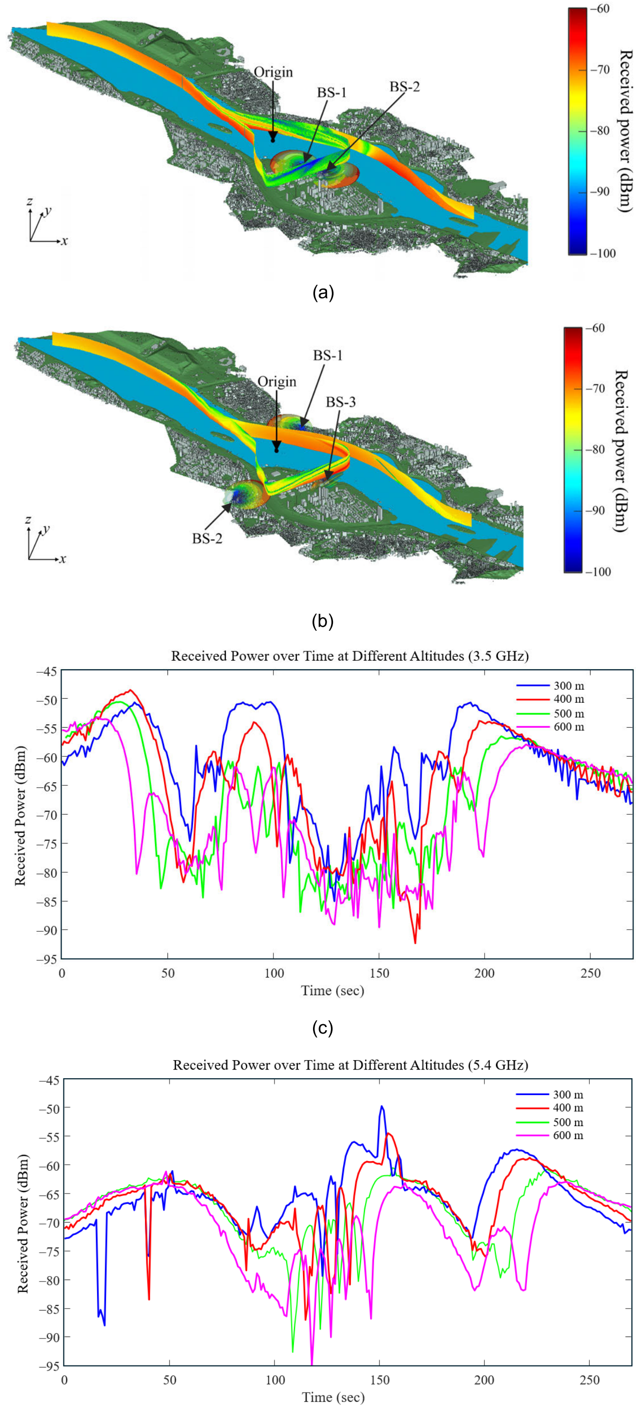

FIGURE 8. Base station deployment optimization and received power of UAM in Yeouido UAM corridor. (a) Optimized 3.5 GHz base stations and received power in UAM corridor. (b) Optimized 5.4 GHz base stations and received power in UAM corridor. (c) Trajectory-based received power analysis at 3.5 GHz. (d) Trajectory-based received power analysis at 5.4 GHz.

Figure 9 shows the analysis to verify the accuracy of the simulation results in the modeled urban environment. To compare the simulation results with measurements, a fixed

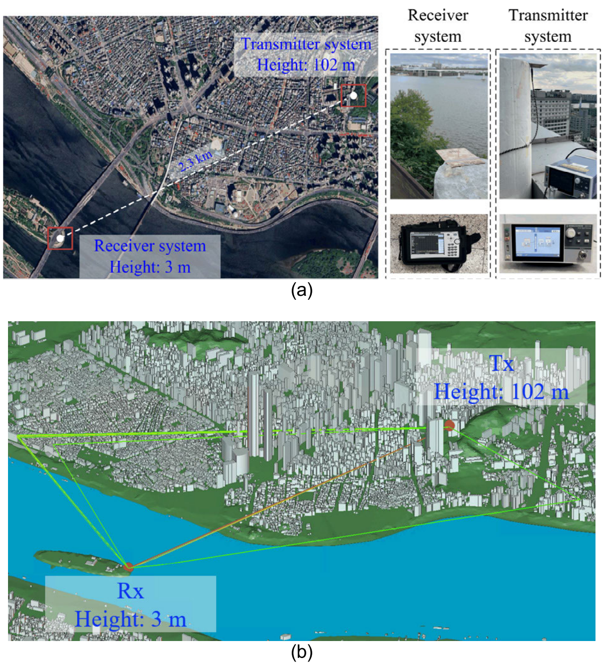

FIGURE 9. 5.4 GHz received power measurement and simulation setup. (a) Measurement of 5.4 GHz along the Han River. (b) Urban environment along the Han River implemented in Wireless InSite.

transmitter and a receiver setup are deployed in a specific area of the modeled urban environment [48], [49]. The transmitter system consists of a monopole antenna, operating at 5.4 GHz, and a signal generator (Rohde & Schwarz SMCV100B). The signal generator transmits the signal with a power of 16 dBm. The receiver system consists of the same monopole antenna and the spectrum analyzer (Anritsu MS-2720T). The locations of the transmitter and receiver are determined to ensure the LOS. The transmitter system is installed on the rooftop of a 102-meter-high building at Hongik University, while the receiver system is located at Seonyudo Park in Yeouido, at a height of 3 meters above sea level. The distance between the transmitter and the receiver system is measured to be 2.3 km, as shown in Figure 9(a). For reliable measurement, the receiver is positioned at four locations spaced 50 cm apart, with two samples collected at each position. The average received power from the resulting eight samples is confirmed to be –110.21 dBm. To compare the results with the theoretical values, the received power is calculated using the following equation [50]:

$$P_r\,(\text{dBm}) = P_t + G_t + G_r - 20\log_{10}\left(\frac{4\pi d}{\lambda}\right) - L_{system} \tag{4}$$

where P_r represents the received power in dBm, and P_t is the transmit power. The antenna gains of the transmitter and receiver are denoted by G_t and G_r, respectively. λ refers to the wavelength, and d is the distance between the transmitter and the receiver. L_{system} is the total system loss, including cable losses at both the transmitter and receiver. Therefore, the theoretical value of the received power using this equation is −110.82 dBm. In the simulation, the Tx and Rx are placed at the same locations as the actual transmitter and receiver systems to obtain received power results, as shown in Figure 9(b). The received power calculated by the Wireless InSite is −110.38 dBm. The similarity between the measurement, theoretical, and simulation values indicates that the simulation results used in the proposed method are reliable for optimizing the deployment of BSs.

IV. CONCLUSION

In this paper, we investigated the method for determining the optimal BS deployment to establish a stable communication environment for UAM operations in urban areas. To model the UAM operating environment realistically, we utilized 1 m resolution DEM files of terrain and buildings which were implemented in the commercial ray-tracing simulation tool, Wireless InSite. In this process, the radiation patterns of the BS's antenna were generated according to the 3GPP-standard, and the receiver antenna patterns were obtained through analysis of the UAM's mounted antenna in commercial EM simulator CST. The proposed method determined the BS locations and the antenna orientation using the GA. In the UAM corridor (an area of approximately 5.4 km^2), the optimization process resulted in the deployment of two base stations at 3.5 GHz with an average received power of −61.36 dBm. At 5.4 GHz, three base stations were deployed with an average received power of −63.74 dBm. This corresponds to a reduction in the number of BSs by 66% at 3.5 GHz and 50% at 5.4 GHz, compared to the conventional six micro-cell BSs deployment. PSO, DE, GWO, and ACO, were also applied to the proposed framework, demonstrating that BS deployment optimization can be effectively performed not only using GA but also with other meta-heuristic algorithms. To ensure the reliability of the simulation, measurements were conducted in an actual urban area. The measurement, theoretical, and simulation values were then compared. The received power values from measurement, theory, and simulation were −110.21 dBm, −110.82 dBm, and −110.38 dBm, respectively. These results demonstrated that the proposed optimization method for BS deployment can be used to establish a stable communication environment in a real UAM corridor.

In future work, we plan to further enhance computational efficiency and solution quality by applying more advanced meta-heuristics, such as MA-HCAGA, MBHGA, and crossover-based PSO. In addition, we will extend our analysis to quantitative UAM performance indicators such as signal quality, channel capacity, and latency under real-time mobility scenarios.

REFERENCES

[1] Z. Wang, D. Delahaye, J.-L. Farges, and S. Alam, "A quasi-dynamic air traffic assignment model for mitigating air traffic complexity and congestion for high-density UAM operations," *Transp. Res. C, Emerg. Technol.*, vol. 154, Sep. 2023, Art. no. 104279.

[2] M. Y. Arafat and S. Pan, "Urban air mobility communications and networking: Recent advances, techniques, and challenges," *Drones*, vol. 8, no. 12, p. 702, Nov. 2024.
[3] H.-J. Moon and C.-B. Chae, "Cooperative ground-satellite scheduling and power allocation for urban air mobility networks," *IEEE J. Sel. Areas Commun.*, vol. 43, no. 1, pp. 218–228, Jan. 2025.
[4] G. Sun, Y. Wang, H. Yu, and M. Guizani, "Proportional fairness-aware task scheduling in space-air-ground integrated networks," *IEEE Trans. Services Comput.*, vol. 17, no. 6, pp. 4125–4137, Nov. 2024.
[5] A. Khoker, B. Mushtaq, M. A. Rehman, and M. J. Abbas, "RF planning and optimization of 5G on the city campus (MUST) of mirpur, Pakistan," *IECE Trans. Sens., Commun., Control*, vol. 1, no. 1, pp. 52–59, Oct. 2024.
[6] H. Yao, Z. Dai, W. Chen, T. Xie, and X. Zhu, "GNSS urban positioning with vision-aided NLOS identification," *Remote Sens.*, vol. 14, no. 21, p. 5493, Oct. 2022.
[7] L. F. P. Martínez, G. Hernández, and D. López, "A model to determine the propagation losses based on the integration of hata-okumura and wavelet neural models," *Int. J. Antennas Propag.*, vol. 2017, pp. 1–8, Jan. 2017.
[8] M. Al-Sahli and N. Gupta, "Improving transmitted signal in wireless body area network transmission using the cost-231 Hata model," *Asian J. Comput. Inf. Syst.*, vol. 2, no. 4, p. 112, Aug. 2014.
[9] S.-S. Oh, J.-W. Choi, D.-W. Kim, Y.-C. Lee, and B.-L. Cho, "Comparison of 0.75–24-GHz reach distances and ratios using propagation path loss measurements from urban and rural line-of-sight environments," *J. Electromagn. Eng. Sci.*, vol. 21, no. 1, pp. 1–7, Jan. 2021.
[10] J. Webber, H. Kamoda, N. Kukutsu, and T. Kumagai, "Millimeter-wave wireless communication in a data center cabinet with adaptive control of propagation," in *Proc. 21st Asia–Pacific Conf. Commun. (APCC)*, Oct. 2015, pp. 272–277.
[11] A. Liu and V. K. N. Lau, "Optimization of multi-UAV-aided wireless networking over a ray-tracing channel model," *IEEE Trans. Wireless Commun.*, vol. 18, no. 9, pp. 4518–4530, Sep. 2019.
[12] C. Pyo, H. Sawada, and T. Matsumura, "A deep learning-based indoor radio estimation method driven by 2.4 GHz ray-tracing data," *IEEE Access*, vol. 11, pp. 138215–138228, 2023.
[13] D. Romero, P. Q. Viet, and R. Shrestha, "Aerial base station placement via propagation radio maps," *IEEE Trans. Commun.*, vol. 72, no. 9, pp. 5349–5364, Sep. 2024.
[14] J. Webber, S. Tsukamoto, S. Ano, N. Kukutsu, and T. Kumagai, "Direction of arrival estimation apparatus for communication based train control system using ESPAR antenna," in *Proc. 3rd Int. Coinf. Digit. Inf. Netw.*, Feb. 2015, pp. 49–54.
[15] Y. Meng, Y. Li, S. Cai, and D. Su, "A dynamic spectrum and power allocation method for co-located pulse radar and communication system coexistence," *Chin. J. Aeronaut.*, vol. 38, no. 4, pp. 1–12, Apr. 2025.
[16] *Remcom Wireless InSite*. Accessed: Mar. 18, 2025. [Online]. Available: http://www.remcom.com/wireless-insite
[17] Y. Yoon and Y.-H. Kim, "An efficient genetic algorithm for maximum coverage deployment in wireless sensor networks," *IEEE Trans. Cybern.*, vol. 43, no. 5, pp. 1473–1483, Oct. 2013.
[18] C. Zuo, X. Zhang, G. Zhao, and L. Yan, "PCR: A parallel convolution residual network for traffic flow prediction," *IEEE Trans. Emerg. Topics Comput. Intell.*, pp. 1–12, 2025.
[19] *3GPP Technical Report 36.814 V9.2.0 Release 9*. Accessed: Mar. 18, 2025. [Online]. Available: https://portal.3gpp.org/
[20] J. Webber, S. Tsukamoto, T. Maeda, T. Kumagai, S. Yamamoto, and S. Aikawa, "Sequentially switched antenna array and application to a Wimax system," in *Proc. 21st Asia–Pacific Conf. Commun. (APCC)*, Oct. 2015, pp. 158–163.
[21] *CST Studio Suite: Electromagnetic Field Simulation Software*. Accessed: Mar. 18, 2025. [Online]. Available: http://www.cst.com
[22] J. Hu, B. Chen, and B. K. Ghosh, "Formation-circumnavigation switching control of multiple ODIN systems via finite-time intermittent control strategies," *IEEE Trans. Control Netw. Syst.*, vol. 11, no. 4, pp. 1986–1997, Feb. 2024.
[23] J. Sarnecki, C. Vinodrai, A. Javed, P. O'Kelly, and K. Dick, "Microcell design principles," *IEEE Commun. Mag.*, vol. 31, no. 4, pp. 76–82, Apr. 1993.
[24] Y. Rong, Z. Xu, J. Liu, H. Liu, J. Ding, X. Liu, W. Luo, C. Zhang, and J. Gao, "Du-bus: A realtime bus waiting time estimation system based on multi-source data," *IEEE Trans. Intell. Transp. Syst.*, vol. 23, no. 12, pp. 24524–24539, Dec. 2022.
[25] *K-UAM Concept of Operations 1.0*. Accessed: Mar. 18, 2025. [Online]. Available: https://www.molit.go.kr
[26] *MOLIT V-World*. Accessed: Mar. 18, 2025. [Online]. Available: https://www.vworld.kr/
[27] A. S. Akopov and L. A. Beklaryan, "Evolutionary synthesis of high-capacity reconfigurable multilayer road networks using a multiagent hybrid clustering-assisted genetic algorithm," *IEEE Access*, vol. 13, pp. 53448–53474, 2025.
[28] A. S. Akopov, "MBHGA: A matrix-based hybrid genetic algorithm for solving an agent-based model of controlled trade interactions," *IEEE Access*, vol. 13, pp. 26843–26863, 2025.
[29] A. P. Engelbrecht, "Particle swarm optimization with crossover: A review and empirical analysis," *Artif. Intell. Rev.*, vol. 45, no. 2, pp. 131–165, Feb. 2016.
[30] D. Cheng, *Fundamentals of Engineering Electromagnetics*. Reading, MA, USA: Addison-Wesley, 1993.
[31] Y. Xi, T. Wang, Y. Wang, H. Zhai, and C. Liu, "A low-profile wideband and dual-polarized antenna with AMC reflector," in *Proc. Int. Conf. Microw. Millim. Wave Technol. (ICMMT)*, Nanjing, China, May 2021, pp. 1–3.
[32] M. Li, Q. Li, B. Wang, C. Zhou, and S. Cheung, "A miniaturized dual-band base station array antenna using band notch dipole antenna elements and AMC reflectors," *IEEE Trans. Antennas Propag.*, vol. 66, no. 6, pp. 3189–3194, Jun. 2018.
[33] Y. Yang, Y. Liang, S. Probsting, P. Li, H. Zhang, B. Huang, C. Liu, H. Pei, and B. R. Noack, "Air taxis-weight, endurance, and range," *Aerospace*, vol. 11, no. 3, p. 200, Mar. 2024.
[34] A. Nikoofard, H. A. Zadeh, and P. P. Mercier, "A 0.6-mW 16-FSK receiver achieving a sensitivity of -103 dBm at 100 kb/s," *IEEE J. Solid-State Circuits*, vol. 56, no. 4, pp. 1299–1309, Apr. 2021.
[35] A. P. Singh, S. Dwivedi, and P. K. Jain, "A novel technique for contrast target detection in through-the-wall radar images," *J. Electromagn. Eng. Sci.*, vol. 22, no. 3, pp. 202–209, May 2022.
[36] *R2022a MATLAB*. Accessed: Mar. 18, 2025. [Online]. Available: https://www.mathworks.com/
[37] K.-K. Yan and Y. Lu, "Sidelobe reduction in array-pattern synthesis using genetic algorithm," *IEEE Trans. Antennas Propag.*, vol. 45, no. 7, pp. 1117–1122, Jul. 1997.
[38] G.-H. Jeon, P. A. Dzagbletey, and J. Chung, "A cross-joint Vivaldi antenna pair for dual-pol and broadband testing capabilities," *J. Electromagn. Eng. Sci.*, vol. 21, no. 3, pp. 201–209, Jul. 2021.
[39] E. Nwelih, J. Isabona, and A. L. Imoize, "Optimization of base station placement in 4G LTE broadband networks using adaptive variable length genetic algorithm," *Social Netw. Comput. Sci.*, vol. 4, no. 2, pp. 1–21, Dec. 2022.
[40] Telecommunications Technology Association (TTA). (Apr. 2024). *TTA Journal, no. 212*. Accessed: May 16, 2025. [Online]. Available: https://www.tta.or.kr/tta/publicationHosuView.do?key=80&rep=1&searchKindNum=1&searchHosu=212
[41] F. Xiong and M. Andro, "The effect of Doppler frequency shift, frequency offset of the local oscillators, and phase noise on the performance of coherent OFDM receivers," NASA Tech. Memo., NASA, Washington, DC, USA, Tech. Rep. NASA/TM-2001-210595, Mar. 2001.
[42] *Specific Attenuation Model for Rain for Use in Prediction Methods*, document Recommendation ITU-R P.838-3, ITU-R, Geneva, Switzerland, Mar. 2005.
[43] M. Song, Y. Huo, Z. Liang, X. Dong, and T. Lǘ, "UAV communication recovery under meteorological conditions," *Drones*, vol. 7, no. 7, p. 423, Jun. 2023.
[44] H. Ganame, L. Yingzhuang, H. Ghazzai, and D. Kamissoko, "5G base station deployment perspectives in millimeter wave frequencies using meta-heuristic algorithms," *Electronics*, vol. 8, no. 11, pp. 1–24, Nov. 2019.
[45] X. Sun, T. Zhang, J. Xu, H. Zhang, H. Kang, Y. Shen, and Q. Chen, "Energy efficiency-driven mobile base station deployment strategy for shopping malls using modified improved differential evolution algorithm," *Appl. Intell.*, vol. 53, no. 2, pp. 1233–1253, Jan. 2023.
[46] A. Gupta, A. Trivedi, and B. Prasad, "B-GWO based multi-UAV deployment and power allocation in NOMA assisted wireless networks," *Wireless Netw.*, vol. 28, no. 7, pp. 3199–3211, Jul. 2022.
[47] J. Tian, M. Gao, and G. Ge, "Wireless sensor network node optimal coverage based on improved genetic algorithm and binary ant colony algorithm," *EURASIP J. Wireless Commun. Netw.*, vol. 2016, no. 1, Apr. 2016.

[48] H.-H. Lee, J. W. Lee, J. H. Kwon, J.-H. Hwang, and C.-H. Hyoung, "Prediction of radio-wave propagation in a shield room: Measurement, simulation, and theoretical method," *J. Electromagn. Eng. Sci.*, vol. 20, no. 1, pp. 45–52, Jan. 2020.
[49] H.-H. Lee, J.-H. Lim, J. W. Lee, J. H. Kwon, J.-H. Hwang, C. H. Hyoung, and H. H. Park, "Estimation of electromagnetic field penetration into concrete buildings using a theoretical approach considering external environmental factors," *J. Electromagn. Eng. Sci.*, vol. 23, no. 3, pp. 212–223, May 2023.
[50] P. K. Bhattacharjee, "Universal law of gravitation compares with electromagnetic waves propagation," *IOSR J. Electron. Commun. Engineering.*, vol. 14, no. 3, pp. 44–48, Jun. 2019.

MINSANG YOON is currently pursuing the B.S. degree in electronic and electrical engineering with Hongik University, Seoul, South Korea. His research interests include machine learning, antenna array, and signal processing for direction finding.

JISEOK PARK received the B.S. degree in electronic and electrical engineering from Hongik University, Seoul, South Korea, in 2025, where he is currently pursuing the M.S. degree. His research interests include reflector antenna, satellite communications, and aircraft airspace analysis.

BOSUNG PARK is currently pursuing the B.S. degree in electronic and electrical engineering with Hongik University, Seoul, South Korea. His research interests include reflector antennas, satellite communications, and direction finding antenna systems.

TAEKYEONG JIN received the B.S. and M.S. degrees in electronic and electrical engineering from Hongik University, Seoul, Republic of Korea, in 2017 and 2019, respectively. He was an Engineer with Hanwha Systems, Gumi, Republic of Korea, from 2019 to 2022. He is currently pursuing the Ph.D. degree in electronic and electrical engineering. His research interests include radar systems, machine learning, array antennas, microwave remote sensing, and electromagnetic wave propagation.

HOSUNG CHOO (Senior Member, IEEE) received the B.S. degree in radio science and engineering from Hanyang University, Seoul, Republic of Korea, in 1998, and the M.S. and Ph.D. degrees in electrical and computer engineering from The University of Texas at Austin, in 2000 and 2003, respectively. In September 2003, he joined the School of Electronic and Electrical Engineering, Hongik University, Seoul, South Korea, where he is currently a Full-Time Professor. His principal areas of research are the use of the optimization algorithm in developing antennas and microwave absorbers. His studies include the design of small antennas for wireless communications, reader and tag antennas for RFID, and on-glass and conformal antennas for vehicles and aircraft.